ACS APPLIED ENERGY MATERIALS
Cite This: ACS Appl. Energy Mater. 2019, 2, 6355−6363
Article
www.acsaem.org

Application of Single-Ion Conducting Gel Polymer Electrolytes in Magnesium Batteries

Laura C. Merrill, Hunter O. Ford, and Jennifer L. Schaefer*

Department of Chemical and Biomolecular Engineering, University of Notre Dame, Notre Dame, Indiana 46556, United States

Supporting Information

ABSTRACT: The development of polymer electrolytes for magnesium batteries has been hindered by difficulties related to achieving sufficient magnesium ion conduction and magnesium electrodeposition. The high charge density of the magnesium cation causes it to interact with both the polar polymer matrix and any counteranions, challenging ion transport. Solvents and salts that are known to be incompatible with the magnesium electrode have widely been used in prior reports to increase ionic conductivity. Herein we report the use of a single-ion conducting magnesium gel polymer electrolyte consisting of a poly(ethylene glycol) dimethacrylate (PEGDMA) crosslinker that is copolymerized with an anionic monomer and subsequently swelled in solvents compatible with magnesium metal. Sufficient magnesium ion conductivities (>10^{-4} S/cm at 25 °C) were able to be achieved with specific solvents and solvent mixtures. Constant potential holds were used to interrogate magnesium electrodeposition from these electrolytes. Small amounts of magnesium deposits were identified; however, the large interfacial impedances appear to impact the degree of deposition. It is hypothesized that the large interfacial impedance is due to the charge transfer resistance associated with the solvated magnesium cation. Thus, it is proposed that the solvated magnesium cation species that is transported in this electrolyte cannot effectively electrodeposit.

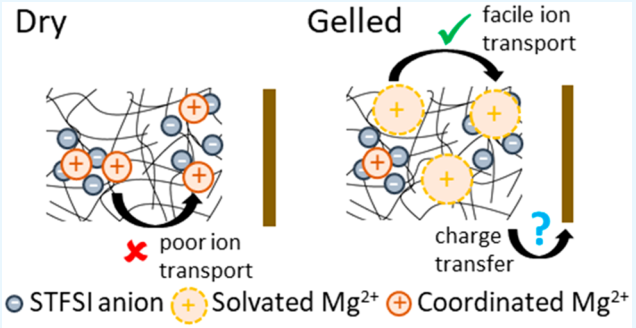

KEYWORDS: *magnesium, batteries, polymer, electrolyte, deposition, conductivity*

1. INTRODUCTION

Demands in high performance battery materials for electric vehicles, portable electronic devices, and grid level storage have led to the development of beyond lithium-ion batteries. Of particular interest is the magnesium anode due to its relatively large theoretical capacity (2200 mAh/g, 3800 mAh/cm^2), its widespread abundance, and increased safety compared to alkali metal anodes. The electrolyte used in combination with a magnesium anode must support reversible electrodeposition and dissolution to enable rechargeability; the electrolyte must be chemically compatible with magnesium metal, mitigating formation of the passivation layer that occurs in the presence of trace impurities, water, and certain solvents/salts. To date, the most successful magnesium electrolyte formulations involve highly flammable and reactive materials or complicated synthetic procedures.[1−6] One option to improve upon the thermal properties of the electrolyte is to use a polymer or gel.

Both gel and solid polymer electrolytes have been researched for use in magnesium metal batteries.[7−11] Because of the higher charge density of Mg^{2+} (approximately twice that of Li^+), the magnesium cation exhibits very strong coordination with polar polymers leading to low cation transference numbers and low cation conductivities.[12,13] Many magnesium polymer electrolyte studies have used magnesium triflate or magnesium bis(trifluoromethanesulfonyl)imide ($Mg(TFSI)_2$), which contains weakly coordinating anions that increase salt dissociation.[9,11,14,15] Computational studies of $Mg(TFSI)_2$ suggest that the $MgTFSI^+$ ion pair is unstable during magnesium electrodeposition, and experimental reports have confirmed that the salt in solution is not chemically stable against magnesium.[16,17] Thus, it is a challenge to enable high Coulombic efficiency magnesium metal deposition and dissolution with electrolytes that employ these salts. Similarly, there are further literature reports on the physical properties of magnesium-based polymer electrolytes containing salts such as $Mg(ClO_4)_2$ and $Mg(NO_3)_2$ or plasticizers such as organic carbonates that are commonly used in Li-ion batteries.[15,18−20] Although all of these works report total ionic conductivity of the prepared electrolyte, magnesium metal electrodeposition or dissolution is not interrogated beyond symmetric cell cyclic voltammetry.[11,19−21] In contrast, reversible electrodeposition/dissolution of magnesium and charge/discharge cycling of a magnesium battery was demonstrated by using a nanocomposite electrolyte of $Mg(BH_4)$-MgO-PEO.[22] The active magnesium cation is hypothesized to be $MgBH_4^+$; reports of analogous glyme-based electrolytes have hypothesized that this cation may further dissociate to Mg^{2+} or that the species in

Received: May 18, 2019
Accepted: August 28, 2019
Published: August 28, 2019

DOI: 10.1021/acsaem.9b00991
ACS Appl. Energy Mater. 2019, 2, 6355−6363

solution is a solvated neutral magnesium borohydride complex (such as $[Mg(BH_4)_2]_2$:3DME or $Mg(BH_4)_2$:diglyme)[22−24]

Magnesium electrodeposition is supported from two types of liquid electrolytes: those where a complex cation is formed, such as $Mg_2(\mu\text{-}Cl)_3^+$, or those that contain magnesium salts that are hypothesized to dissociate in an ether to result in free monovalent anions, solvated Mg^{2+}, and potentially contact ion pairs.[25] Complex electrolytes contain large amounts of chloride which is corrosive to common current collectors. Despite this, the complex electrolytes have had much success in the magnesium battery field in terms of reversibility, but the best efficiencies have been achieved using the volatile solvent tetrahydrofuran (THF).[2,26] Simple salt electrolytes containing bulky boron-based anions such as carboranes or fluorinated boron-based anions like $Mg(B(hfip)_4)_2$, Mg-FPB, and Mg-$(TPFA)_2$ have shown reversible electrodeposition in glyme-based solvents, including tetraglyme.[4,5,27−29] The active species for these systems with bulky anions is hypothesized to be a glyme solvated Mg^{2+} cation.

A small number of polymer electrolytes have been demonstrated where an electrolyte that supports reversible deposition is integrated into the polymer. Aurbach and co-workers used a Grignard based electrolyte, $Mg(AlCl_2EtBu)_2$ in tetraglyme, with PVDF and PEO.[7] This provided a route to achieve magnesium electrodeposition with increased thermal stability. Cui and co-workers showed that reversible deposition could be achieved from a polyTHF gel polymer electrolyte with $Mg(BH_4)_2$ and $MgCl_2$.[30] The use of ionomer materials has been employed in magnesium/sulfur systems as a separator that can both sterically and electrostatically reject polysulfides.[31] In each of these cases, the polymer may help to increase thermal stability, but ultimately acts as a passive support or separator material rather than as the active medium for the magnesium cation conduction.

Single-ion conductors have become a popular approach to polymer electrolytes within the lithium-based battery field.[32−35] The immobilization of the anion, by covalently binding it to the polymer backbone, allows for cation transference numbers approaching unity. A high cation transference number mitigates the formation of concentration gradients across the electrolyte, which reduces interfacial impedance and the propensity for dendritic metal growth.[36] There has been minimal research in single ion conducting polymers for application in magnesium batteries. The Balsara group demonstrated single-ion conducting block copolymer electrolytes based on both lithium and magnesium; the magnesiated polymers exhibited conductivities 1−2 orders of magnitude less than the lithium analogues.[8] In our previous work, multivalent ions generally had a decrease in conductivity by 2 orders of magnitude compared to monovalent ions (Li^+, K^+) in a solvent-free, single-ion conducting PEO-based matrix.[29] This further demonstrates that the magnesium cation is less mobile in dry polymers in part due to its increased binding energy. To our knowledge, there has not been a reported investigation of magnesium electrodeposition from an organic, single-ion conducting electrolyte.

Herein we investigate the use of cross-linked, single-ion conducting gel polymer electrolytes for magnesium batteries. Furthermore, we probe the potential of a solvated magnesium cation (i.e., Mg^{2+}:3DME) to electrodeposit. We first discuss the use of organic solvents to dissociate the magnesium cation from the polymer and enable sufficient magnesium cation transport (10^{-4} S/cm). Then, magnesium electrodeposition from the ionomers was attempted through both galvanostatic and potentiostatic holds. A small amount of magnesium deposition onto a copper substrate was confirmed via microscopy and elemental mapping; however, the electrodeposition of magnesium from the single-ion conducting gel electrolyte is hypothesized to be limited by a high charge transfer resistance.

2. EXPERIMENTAL SECTION

2.1. Chemicals. Tetrahydrofuran (THF), 1,2-dimethoxyethane (DME), diethylene glycol dimethyl ether (diglyme), tetraethylene glycol dimethyl ether (tetraglyme), and dimethyl sulfoxide (DMSO) were purchased from Sigma-Aldrich and were dried on molecular sieves prior to use. Sulfolane (SL) and butyl sulfone (BS) were purchased from Sigma-Aldrich and distilled before use. Poly(ethylene glycol) dimethacrylate (MW of 1000 g/mol, PEGDMA 1000) was purchased from Polysciences and used without any further purification. Potassium 4-styrenesulfonyl(trifluoromethylsulfonyl)-imide (KSTFSI) was synthesized as described in previous reports.[32,34]

2.2. Polymer Synthesis. PEGDMA 1000 was copolymerized with the KSTFSI monomer in a DMSO solution under UV light irradiation for a total of 45 min. The monomer solution was sandwiched between two glass plates with a glass coverslip used as a spacer. The monomers were mixed in DMSO (0.7 g monomer/mL DMSO) at a ratio of 20 ethylene oxide (EO) units per STFSI anion (20 EO:Ch). The photoinitiator used was 2-hydroxy-4'-(2-hydroxyethoxy)-2-methyl-propiophenone (Sigma-Aldrich). After polymerization, the films were ion exchanged to the magnesium form via exposure to a solution of 0.5 M $MgCl_2$ in deionized water for 48 h with this solution being changed out every 12 h. Then, excess salt was removed via soaking the films in pure deionized water for 48 h, with replacement of the water bath every 12 h. Polymer films were dried at 80 °C under vacuum for 16 h and stored in an argon-filled glovebox. The thickness of the dry films was around 110 μm. The magnesium content of the films was confirmed to be stoichiometric (1 Mg^{2+} per 2 STFSI− units) and the potassium content was confirmed to be negligible, indicating complete ion exchange, via inductively coupled plasma optical emission spectroscopy (ICP-OES). Details of the ICP-OES methods and results can be found in the Supporting Information (Figure S1, Table S1, and Table S2).

2.3. Small-Angle X-ray Scattering (SAXS). SAXS measurements were obtained at the Advanced Photon Source (beamline 12-ID-B) at Argonne National Lab. An X-ray beam wavelength of 0.9322 Å (photon energy 13.3 eV) was used to take measurements. A silver behenate standard was used to calibrate the q-range. Samples were loaded into glass or quartz capillary tubes (Charles Supper Company) in an argon atmosphere and sealed with wax. The raw data were background corrected and analyzed by using the Igor Pro-Irena SAS package.

2.4. Conductivity Measurements. Films were swelled in each solvent, or solvent mixture, for 4 h in an argon glovebox to ensure the films were fully equilibrated in the solvent prior to impedance spectroscopy. Swelling ratios as a function of time for select solvents are shown in Figure S2, and solvent specific swelling ratios at the 4 h time point can be found in Table S3. The swelled films were loaded into a symmetric cell with brass electrodes inside the glovebox. The sample cell was then transferred into the sample holder of the Novocontrol broadband dielectric spectrometer with a Quatro temperature control unit for conductivity measurements. The measurements were acquired in the temperature range of 0 and 100 °C, as appropriate for each solvent using an AC voltage of 0.1 V_{rms} in the frequency range of 10^7−0.1 Hz.

2.5. Electrochemistry Measurements. Constant potential deposition measurements, and the corresponding impedance spectroscopy measurements, were taken using a PARSTAT MC1000 (Princeton Applied Research). For constant potential deposition measurements, a potential of −700 mV vs Mg^{2+}/Mg^0 was applied for 10 h. Impedance measurements were taken before and after the constant potential holds over the frequency range of 10000 and 1 Hz

DOI: 10.1021/acsaem.9b00991
ACS Appl. Energy Mater. 2019, 2, 6355−6363

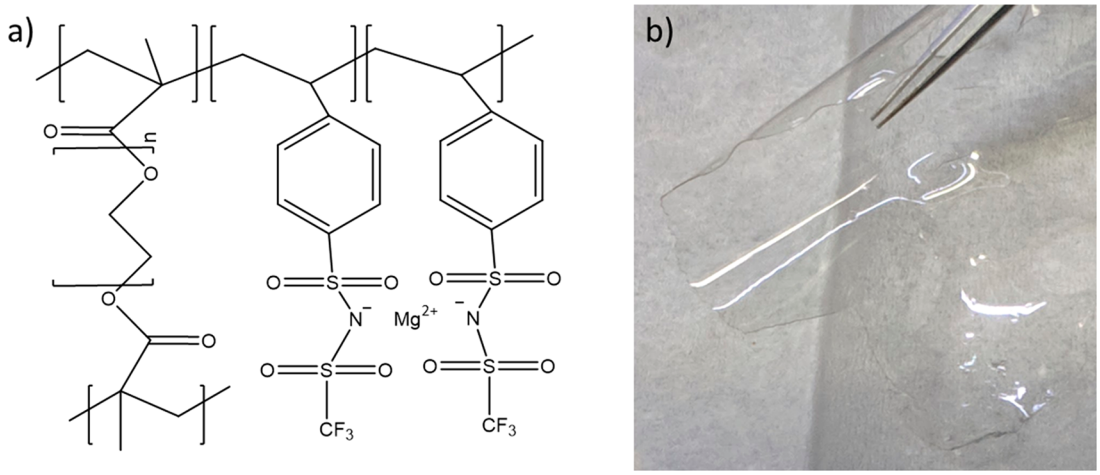

Figure 1. (a) Structural schematic of the statistically copolymerized and magnesiated P(PEGDMA)−P(STFSI) network. (b) Image of the freestanding polymer film.

at 10 V_{rms}. This measurement was taken by using both asymmetric (Mg/Cu) and symmetric (Mg/Mg) CR2032 coin cell configurations. Magnesium was purchased from Solution Materials, LLC, and the oxide layer was scraped off before use. Copper was purchased from McMaster Carr and was cleaned with isopropanol prior to use.

2.6. Scanning Electron Microscopy/Energy Dispersive X-ray Spectroscopy (SEM/EDS). Electrode samples were washed with anhydrous THF and dried under vacuum before SEM/EDS measurements. Samples were transported to the electron microscope via a PELCO vacuum pin stub holder to minimize air exposure. Electron micrographs were taken with a Magellan 400 SEM (FEI). Measurements were taken at 10 kV and 50 pA at a working distance of 4.3 mm. A Bruker spectrometer was used to take EDS measurements for which the voltage was kept constant but the current was increased until adequate signal was achieved (>1000 cps).

2.7. X-ray Photoelectron Spectroscopy (XPS). XPS measurements were taken by using a PHI Versa Probe II spectrometer. Samples were washed with THF, dried under vacuum prior to measurement, and transported to the instrument by using the same PELCO sample holder. Air exposure could not be avoided upon transfer of the sample from the PELCO holder into the instrument. Samples were sputtered for 2 min with 2 kV Ar^+ to remove some oxidation resulting from the transfer. Point measurements were taken by using 50 W X-rays. Each chosen binding energy was taken with a 23.5 eV pass energy with a 100 ms time step over 12 scans.

3. RESULTS AND DISCUSSION

3.1. Magnesium Cation Conduction. Achieving sufficient (10^{-4} S/cm) cation conductivities in single-ion conductors is challenging. Previous works have shown that conductivity of a cross-linked solvent-free ionomer can be improved by changing the counteranion chemistry, the cross-linker chain length, and charge density. In this work, these variables were kept constant, and the film was swelled in a variation of solvents to promote the dissociation of magnesium. The magnesium cation is very stable within the polymer matrix, coordinated by both ether oxygens and anions, effectively creating ionic aggregates. The STFSI anion chemistry was chosen due to its lower binding energy.[32,33] The electron-withdrawing nature of the groups on the anion distributes the negative charge. Figure 1 shows the chemistry of the statistically copolymerized network alongside an image of the cross-linked polymer film. The magnesium cation can coordinate with two STFSI anions, which can effectively create aggregation within the polymer. As shown, the cross-linked polymer is a colorless, freestanding film.

Magnesiated ionomer films were swelled in a variety of pure solvents and solvent mixtures to promote magnesium dissociation and transport. Table 1 outlines properties of the different solvents used, including donor number and dielectric constant. Ethereal solvents were chosen for study as they are typically used in liquid magnesium electrolytes and have been shown to be stable against the magnesium surface. As previously discussed, glymes are hypothesized to effectively solvate a magnesium cation to form an electrochemically active Mg^{2+} species. By using a single-ion conductor, this hypothesis can, in theory, be tested directly as the anions cannot contribute to the measured dc ionic conductivity. In addition to ethers, more polar solvents such as sulfones and DMSO were also used. Sulfones in particular have gained recent interest in the literature for magnesium battery applications due to their increased thermal stability.[37,38] It is noted that DMSO has been predicted to be chemically and electrochemically stable against magnesium metal at relevant potentials; however, the limited experimental studies are inconclusive regarding the stability of DMSO against the magnesium anode.[39−41] It is noted that the strong solvating ability of solvents with high donor numbers, such as DMSO, can make desolvation unfavorable, therefore inhibiting deposition.[39,40,42] Despite this, irreversible deposition and solvent decomposition have been observed with solvents such as sulfolane, which has the lowest donor number listed in Table 1.[37,43] Generally, magnesium deposition appears to be sensitive to the coordination environment, suggesting that the donor number

Table 1. Properties of Solvents Used To Swell the Magnesium Gel Polymer Electrolytes (NR Refers to "Not Reported")

solvent	boiling point (°C)	melting point (°C)	dielectric constant	donor number
THF	66	−108.4	7.52	20
DME	85	−58	7.3	20
diglyme	162	−64	7.23	18
tetraglyme	275	−30	7.79	12
butyl sulfone	290	44	27	NR
sulfolane	285	27.5	44	14.8
dimethyl sulfoxide	189	19	46.7	29.8

DOI: 10.1021/acsaem.9b00991
ACS Appl. Energy Mater. 2019, 2, 6355−6363

provides the strongest indicator of overall performance while dielectric constant may provide the best indicator for conductivity.

Demonstrated in Figure 2, the conductivity of the dry ionomer is abysmal, on the order of 10^{-9} S/cm at temperatures

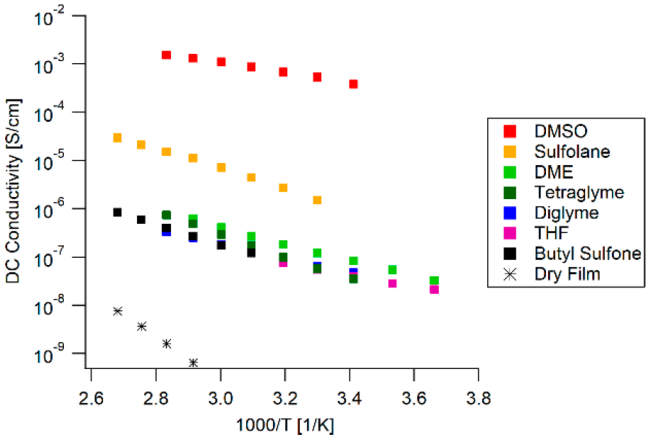

Figure 2. The DC ionic conductivity as a function of temperature of the single-ion conducting magnesium gel polymer electrolytes swelled in pure solvents.

above 80 °C. This is a conductivity of 2 orders of magnitude less than the block copolymer developed by Balsara and co-workers, presumably due to the decreased mobility of the poly(ethylene glycol) chains due to cross-linking.[8] With the addition of solvents, the cation conductivity increases as shown in Figure 2. The molar conductivity of the swelled polymer films, which accounts for differences in charge carrier density due to differences in swelling ratios, is shown in Figure S3. Neither the magnitude of the donor number nor the dielectric constant of the solvent directly tracks with the increase in conductivity. However, it can be used as a rough indicator where higher dielectric constant may result in higher ionic conductivity; similar results have been found for other solvated ionomers, such as Nafion.[40,44,45]

DMSO is known to have the ability to separate ion pairs; therefore, unsurprisingly the polymer swelled in DMSO has the highest conductivity, on the order of 10^{-4} S/cm. This is the same order of magnitude of conductivity reported for various liquid magnesium electrolytes.[37] The neat ethereal solvents and the butyl sulfone show some ability to facilitate magnesium cation transport, albeit at a much lower level than the DMSO and sulfolane.

In an attempt to promote both ion dissociation and the formation of an electrochemically active species, the polymer films were swelled in solvent mixtures. The corresponding conductivity data are shown in Figure 3. It is observed that mixing the sulfone or sulfoxide solvents with ethereal solvents extends the temperature range over which the solvent is in the liquid phase, facilitating ion transport. There is a slight overall increase in conductivity by adding sulfolane to the ethers; however, the most significant increase in conductivity is again observed with the addition of DMSO. At 10 vol % DMSO (balance THF or DME; termed 90 DME/10 DMSO), conductivities on the order of 10^{-4} S/cm are still able to be achieved. This shows that only a small amount of DMSO is needed to actually dissociate the majority of the magnesium and enable its transport. In our previous work, we

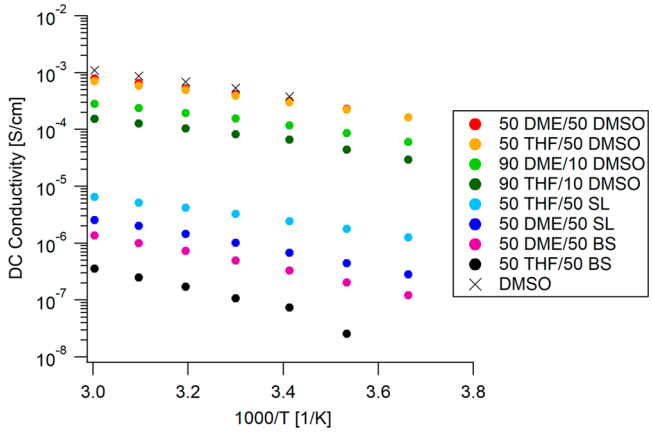

Figure 3. The DC ionic conductivity as a function of temperature of the single-ion conducting magnesium gel polymer electrolytes swelled in mixed solvents.

demonstrated that a cosolvated complex magnesium cation ($Mg_2Cl_3^+$) was able to reversibly deposit magnesium metal.[37] With this work, we attempt a similar approach to deposit magnesium using solvent mixtures in films, only this time with the "simple" Mg^{2+} species.

To fully understand the impact of solvent on conductivity, it is important to understand the impact of solvent on the network structure. In cross-linked PEGDMA systems, acrylate backbone segments segregate into spatially homogeneous regions with higher X-ray scattering length density than PEG-rich regions.[46] Via the use of the Bragg's condition, where $q_x = 2\pi/d_x$, the distance between structures responsible for scattering, d_x, can be calculated from the local maximum q_x in small-angle X-ray scattering (SAXS) spectra.[47] As ionic monomer moieties are incorporated in the network, they are located along the acrylate backbone and undergo a similar segregation process in which ionic aggregates are formed.[31,47−49] Figure 4 shows the SAXS spectra of the magnesiated polymer electrolytes swelled in the different solvents and solvent mixtures in addition to PEGDMA polymers without STFSI. The polymer samples that contain no STFSI display a local maximum corresponding to the acrylate-rich region spacing. As the ionic units are incorporated, the local maximum shifts to smaller q, indicating a larger distance between scattering structures, and the intensity of the maximum is increased, indicating that there is a greater contrast between more strongly scattering structures and the surrounding medium.

The local maximum in the STFSI-containing polymers, known as the "ionomer peak", is indicative of ionic aggregation. In ethereal solvents, a characteristic length scale q_1 of 5.2 nm is evident, whereas with the film swelled in DMSO, the characteristic length scale q_2 between contrasting features is lower at 4.2 nm even though the swelling ratio is higher. Samples swelled in solvent mixtures display characteristic length scales in between these two extremes. A smaller length scale between aggregates indicates a smaller aggregate size, with aggregate size inversely correlated to the degree of ion dissociation within the network.[31] Hence, the DMSO swelled samples have a higher degree of ion dissociation compared to samples swelled with ethereal solvents. Further evidence of the differences in ionic aggregation between ether-based and DMSO-based networks is seen by comparing the ionomer network scattering peak intensity with that of the ion-

DOI: 10.1021/acsaem.9b00991
ACS Appl. Energy Mater. 2019, 2, 6355−6363

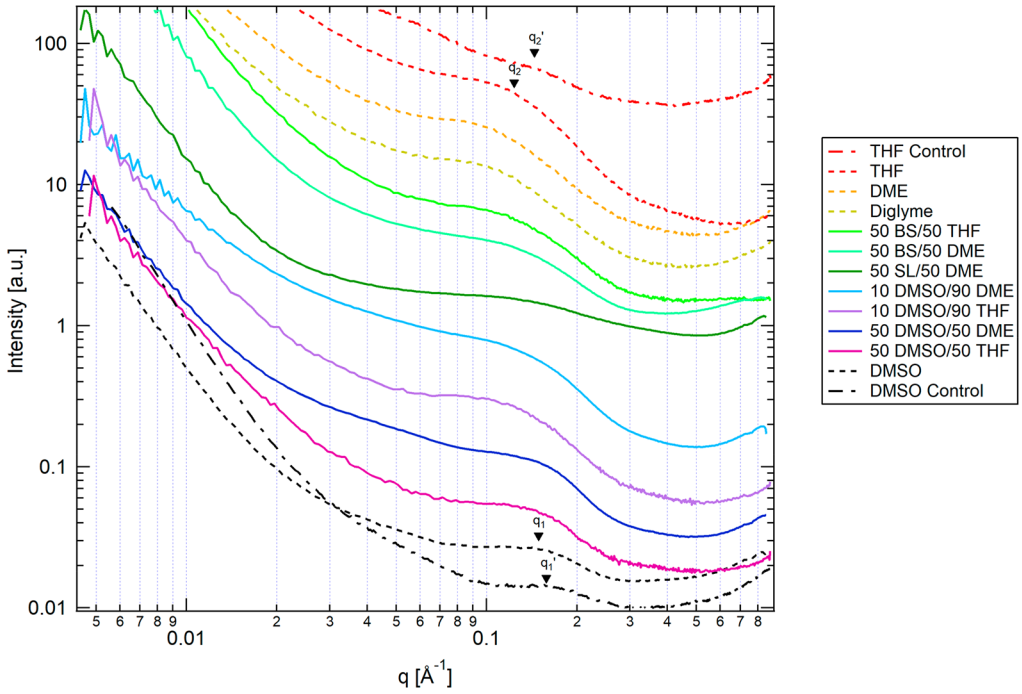

Figure 4. SAXS spectra of cross-linked single-ion conducting magnesium polymer gel electrolytes swelled in different solvents (dashed lines) and solvent mixtures (solid lines). The red and black dot-dashed lines note a cross-linked PEGDMA network (without any tethered salt) swelled in THF and DMSO, respectively. q_2 and q_2' denote the scattering peak in the THF swelled case with and without the tethered anion, respectively, and q_1 and q_1' denote the scattering peak for the polymer swelled with DMSO with and without the tethered anion. The local maxima in the spectra is characteristic of ionic aggregation.

free gels; for THF swelled gels, incorporation of ionic moieties in the networks results in a larger increase in scattering peak intensity as the aggregation is more severe.

Dissociation of ionic aggregates dramatically impacts observed conductivity in two ways. First, a greater dissociation of ionic aggregates results in a greater number of charge carriers which increases the conductivity. Second, increased dissociation improves ion mobility. Through the extensive study of the transport properties of similar materials, we have shown previously that highly aggregated polymers are more rigid with a more tortuous diffusion/electromigration pathway for solvated species.[31] The reduction in ionic aggregation due to the DMSO induced ion dissociation allows for more facile magnesium transport, therefore leading to an enhancement in the conductivity.

The absolute intensity of the scattering peaks cannot be fairly compared between gels based on different solvents, as the change in solvent also effects the degree of contrast between the ionic aggregates and the surrounding matrix. Nonetheless, the change of solvent clearly affects the electrolyte structure, with the polymer gels based on mixed solvents exhibiting intermediate structural changes. These structural differences in part dictate the material transport properties and performance characteristics.

3.2. Electrodeposition of Magnesium. For these polymer gel electrolytes to be practically used in a rechargeable magnesium metal battery, there must be sufficient conductivity of the cations as well as reversible magnesium electrodeposition and dissolution of magnesium. Therefore, we investigated magnesium deposition from the polymer gel electrolytes based on DMSO and the 90 DME/10 DMSO mixture, as high ionic conductivity was achieved in both cases. It was anticipated that the film swelled with 90% DME may have some amount of DME solvated magnesium cations, which are predicted to be the active species that electrodeposits magnesium.[4,6] From the cyclic voltammetry measurements shown in Figure S4 for the DMSO swelled film, a slight amount of negative current may be observed, but it is inconclusive whether this is due to metal deposition or electrolyte decomposition. Despite the high ionic conductivity of these electrolytes, a constant current of −0.01 mA/cm^2 was not able to be supported at reasonable potentials; rather, the cell potential decreased to a potential within the range of solvent decomposition (see Figure S5). The current transient shows multiple processes, including a short plateau around −700 mV vs Mg^{2+}/Mg^0, and then two separate slopes, followed by a plateau at −1.4 V vs Mg^{2+}/Mg^0. The short hold may be related to the deposition of ions at the interface, and the two slopes suggest two separate electrochemical reactions, likely associated with parasitic decomposition reactions. This suggests that substantial magnesium electrodeposition cannot be achieved through galvanostatic methods, perhaps due to the strongly coordinated DMSO or a large charge transfer resistance. However, by applying a constant potential of −700 mV vs Mg, a constant negative current ranging from 0.05 to 0.1 mA/cm^2 was able to be maintained as shown in Figure S6. The absolute value of these currents suggests faradaic reactions.

Upon imaging of the electrodes, small and dispersed deposits were observed from both the 90 DME/10 DMSO and DMSO swelled electrolytes. These deposits are globular in shape and sporadically present on the copper current collector. The elemental mapping of the magnesium deposit from the 90 DME/10 DMSO swelled film showed there was some organic decomposition on the deposit, represented by an increased concentration of oxygen and carbon in the region of the

DOI: 10.1021/acsaem.9b00991
ACS Appl. Energy Mater. 2019, 2, 6355−6363

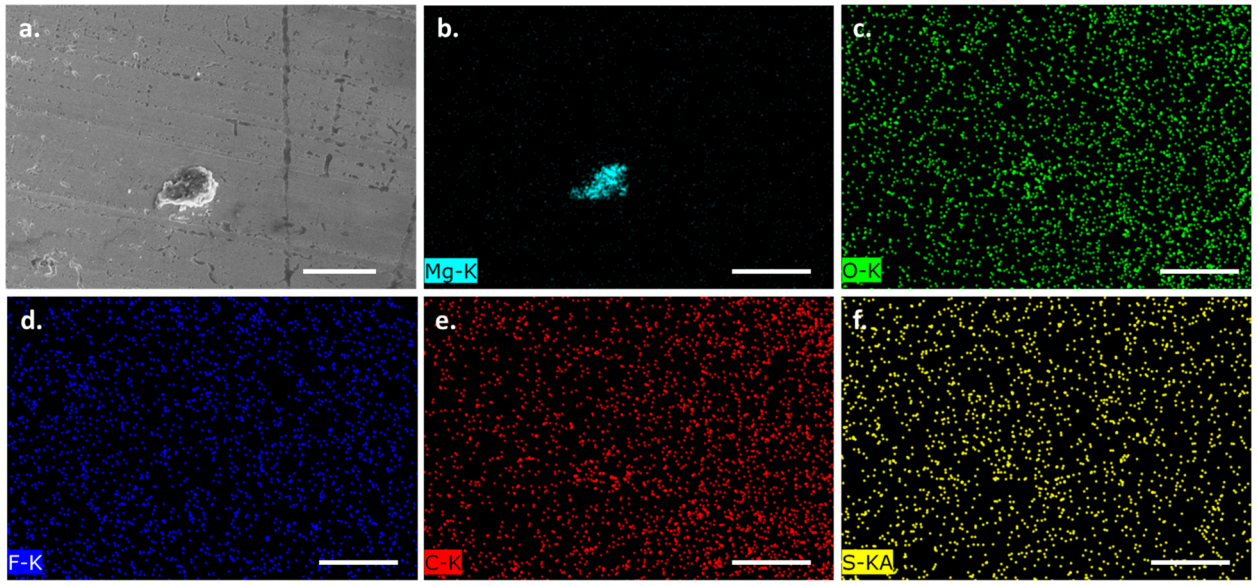

Figure 5. SEM/EDS of a magnesium-rich deposit on copper from the 90 DME/10 DMSO swelled polymer electrolyte film: (a) SEM image of deposit; (b) magnesium elemental mapping, teal; (c) oxygen elemental mapping, green; (d) fluorine elemental mapping, blue; (e) carbon elemental mapping, red; (f) sulfur elemental mapping, yellow. The scale bar indicates 20 μm.

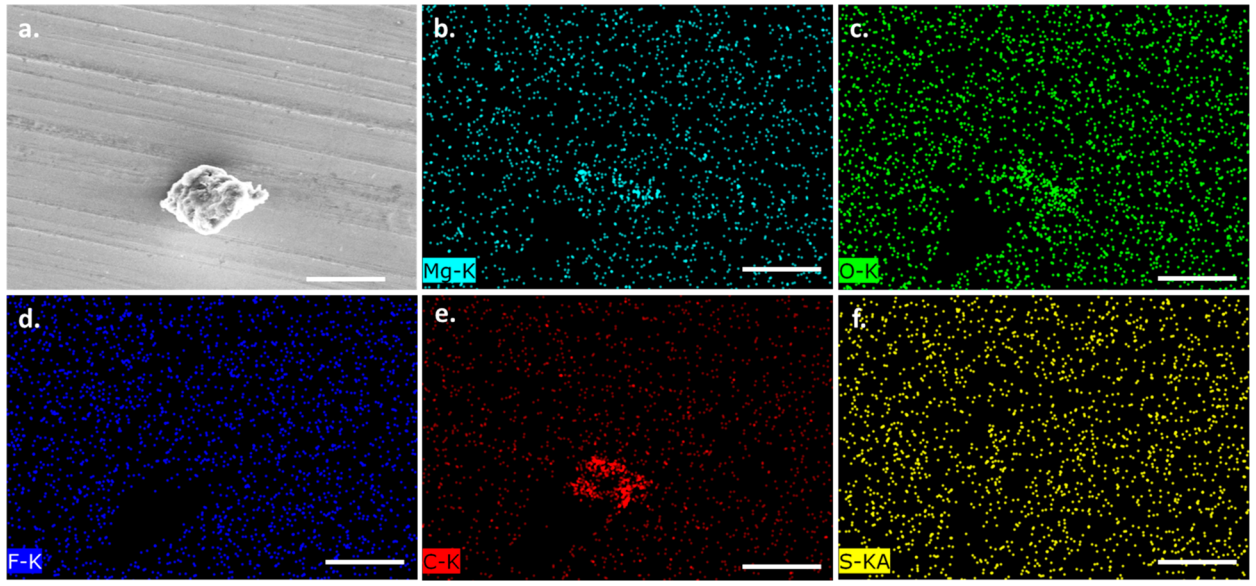

Figure 6. SEM/EDS of a magnesium-rich deposit on copper from the DMSO swelled polymer electrolyte film: (a) SEM image of deposit; (b) magnesium elemental mapping, teal; (c) oxygen elemental mapping, green; (d) fluorine elemental mapping, blue; (e) carbon elemental mapping, red; (f) sulfur elemental mapping, yellow. The scale bar indicates 20 μm.

deposit as shown in Figure 5. The elemental mapping shows that the magnesium is concentrated in the area that the deposit is present. In contrast, the deposit that is obtained by using the purely DMSO swelled electrolyte showed a higher relative amount of decomposition products and charging, as shown in Figure 6. The charging is evident from the black space in the EDS map and indicates a greater concentration of electrically insulative compounds (representative of decomposition products). This is further evident from the higher proportion of oxygen and carbon on in the EDS mapping. Unlike when using the 90 DME/10 DMSO swelled electrolyte, the magnesium mapping is spread out beyond the concentrated area. This suggests either more very small magnesium nucleation sites or a greater number of decomposition products on the copper electrode. DMSO has a stronger coordination with the magnesium cation than DME; therefore, a greater number of decomposition products would be expected as a result of the desolvation process. This corresponds with the elemental mapping. As substrate type can effect electrodeposition, the same deposition test was performed on a scraped magnesium working electrode, and the results are appended in the Supporting Information (Figures S7–S9). Despite a current of 0.05 mA/cm^2 being maintained throughout the 10 h hold, magnesium deposition was not obvious.

Because the amount of magnesium actually deposited on the copper electrodes in each case is very small, neither XPS nor XRD could be used to confirm that the deposit observed in the

DOI: 10.1021/acsaem.9b00991
ACS Appl. Energy Mater. 2019, 2, 6355–6363

EDS is indeed metallic magnesium. To determine the degree of decomposition that results from the electrochemical measurements on the polymer gel electrolytes in contact with magnesium metal, XPS measurements were taken of the magnesium working electrodes from symmetric cell measurements. The same constant potential method was applied for symmetric cells, and characterization was performed on the working electrode.

Figure 7 shows the Mg 2p region of the XPS spectra for each electrode. Both magnesium electrodes that endured the

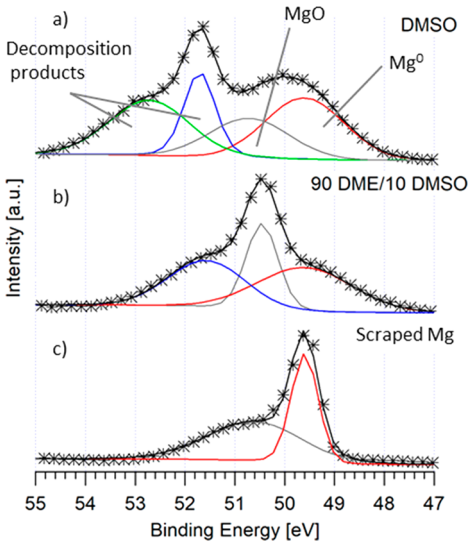

Figure 7. Mg 2p region of XPS spectra for the Mg working electrode from an Mg/Mg cell containing (a) a film swelled in DMSO only, (b) a film swelled in 90 DME/10 DMSO, and (c) magnesium sheet that was scraped to remove the oxide layer and washed with anhydrous THF.

constant potential hold in contact with a polymer gel electrolyte have a greater degree of oxidation compared to the freshly scraped electrode. In the Mg 2p region of the XPS spectra, there are two peaks representative of decomposition products. Considering the XPS spectra of other elements (shown in Figure S10), it is likely that there is a metal fluoride present on the surface of the electrode for both the DMSO and 90 DME/10 DMSO cases. This suggests that the anion was able to decompose at on the metal surface. $Mg(TFSI)_2$ is known to be unstable against magnesium metal, and experimental studies of $Mg(TFSI)_2$ electrolytes have shown MgF_2 as a resultant decomposition product.[17,41] Given that the STFSI and TFSI anions are chemically similar, it is likely that anions at the interface were able to react with the magnesium metal. The electrode in contact with the DMSO swelled polymer exhibits another peak within the magnesium region evident of further decomposition products. The exact chemistry could not be identified; however, past studies of DMSO with magnesium batteries have suggested that DMSO can lead to passivation of the magnesium electrode.[39] Therefore, this is likely representative of an irreversible reaction between DMSO and magnesium that occurs when DMSO-solvated Mg^{2+} cations reach the electrode surface.

Impedance measurements were taken before and after the constant potential holds, and the spectra and corresponding fits from the symmetric cells are shown in Figure 8. The fit parameters are appended in the Supporting Information

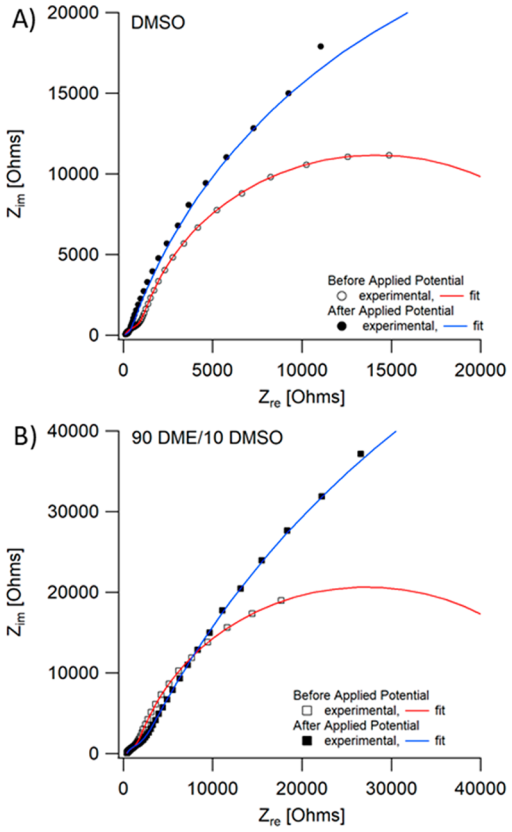

Figure 8. Impedance spectra of Mg/Mg cells with a (a) DMSO and a (b) 90 DME/10 DMSO swelled polymer electrolyte film. Impedance spectra are shown before and after the applied potential hold.

(Table S4). Each impedance response can be approximated with an R(QR)(QR) circuit, as suggested by the two semicircles. The first semicircle is at a moderate impedance; however, the second semicircle indicates an immense interfacial impedance. Because the conductivity of both electrolytes is adequate and the swelled films have good contact with the magnesium electrodes, it is hypothesized that there is a large charge transfer resistance that is represented by the second semicircle. The first semicircle may be due to an interfacial impedance such as a boundary layer effect, given the order of magnitude (thousand(s) of ohms). Figure S11 shows an expanded view of the first semicircle. The mixed solvent electrolyte generally results in greater impedances compared to the DMSO-only electrolyte. The initial shift in impedance is caused by changes in the bulk resistance, reflected in the differences in conductivity. However, the exact reason for the increased interfacial impedance for the mixed solvent case could not be determined. Because it is hypothesized that the large interfacial impedance is due to a charge transfer resistance, it is suggested that the cosolvated, or DME solvated, Mg^{2+} may not be able to aptly participate in electrochemical reactions. After the constant potential hold, the impedance increased for both cases. Any sort of decomposition on the magnesium surface could lead to this increase.

We were able to confirm that the presence of the large impedance is not due to the DMSO by repeating the measurement with a DME swelled film, as shown in Figure S12. The same very large interfacial impedance is observed, indicating that the large resistance is not due to the presence of

DOI: 10.1021/acsaem.9b00991
ACS Appl. Energy Mater. 2019, 2, 6355−6363

the DMSO or any DMSO decomposition. It is known that the high charge density of Mg^{2+} can lead to difficulties with reversible deposition; thus, it is predicted that the large charge transfer resistance associated with desolvation of Mg^{2+} is related to this large impedance. It is also possible that there is a large resistance associated with electrodissolution of magnesium into the single-ion conducting polymer electrolyte. Impedance analysis of cells containing polymer films swelled in electrolytes with free salt do not show this same large impedance, suggesting that it is the presence of mobile anions that affect the magnesium complexation that allows for more facile electrodeposition and dissolution. Despite the large resistance, it is feasible that a solvated Mg^{2+} cation can deposit, given the small but finite amounts of magnesium-rich solid deposition products observable via electron microscopy.

4. CONCLUSIONS

We conclude that single ion conducting polymers swelled with specific solvents can conduct magnesium ions at sufficient rates. However, despite being able to achieve adequate magnesium conductivity (>10^{-4} S/cm at room temperature), magnesium deposition from the solvated cation (or dissolution into the electrolyte) remains the primary challenge. Only small amounts of isolated magnesium deposits were observed via electron microscopy. We hypothesize that the large charge transfer resistance associated with desolvation of Mg^{2+} is responsible for this result. Although cation conductivity may be improved by changing the polymer chemistry, it is likely that this large charge transfer resistance will remain unless an additional species is added that stabilizes an active magnesium cation complex at the electrode−electrolyte interface.

■ ASSOCIATED CONTENT

Supporting Information

The Supporting Information is available free of charge on the ACS Publications website at DOI: 10.1021/acsaem.9b00991.

Further electrochemical characterization of the films, impedance fit parameters, and appended XPS data (PDF)

■ AUTHOR INFORMATION

Corresponding Author

*E-mail: Jennifer.L.Schafer.43@nd.edu.

ORCID

Jennifer L. Schaefer: 0000-0003-4293-6328

Funding

Laura C. Merrill acknowledges ND Energy and the Notre Dame Center for Environmental Science and Technology for financial support. This work was supported by funding from the National Science Foundation under Award CBET-1706370.

Notes

The authors declare no competing financial interest.

■ ACKNOWLEDGMENTS

We thank the Notre Dame Materials Characterization Facility, the Notre Dame Center for Environmental Science and Technology, and the Notre Dame Integrated Imagining Facility for use of their facilities and instrumentation. We also thank Dr. Xiaobing Zuo from Argonne National Laboratory for his assistance with collecting SAXS spectra. This research used the facilities at the Advanced Photon Source, a U.S. Department of Energy (DOE) Office of Science User Facility at Argonne National Laboratory under Contract DE-AC02-06CH11357.

■ REFERENCES

(1) Yoo, H. D.; Shterenberg, I.; Gofer, Y.; Gershinsky, G.; Pour, N.; Aurbach, D. Mg Rechargeable Batteries: An On-Going Challenge. *Energy Environ. Sci.* **2013**, *6*, 2265−2279.

(2) Mohtadi, R.; Mizuno, F. Magnesium Batteries: Current State of the Art, Issues and Future Perspectives. *Beilstein J. Nanotechnol.* **2014**, *5*, 1291−1311.

(3) Mizrahi, O.; Amir, N.; Pollak, E.; Chusid, O.; Marks, V.; Gottlieb, H.; Larush, L.; Zinigrad, E.; Aurbach, D. Electrolyte Solutions with a Wide Electrochemical Window for Rechargeable Magnesium Batteries. *J. Electrochem. Soc.* **2008**, *155*, A103−A109.

(4) Tutusaus, O.; Mohtadi, R.; Arthur, T. S.; Mizuno, F.; Nelson, E. G.; Sevryugina, Y. V. An Efficient Halogen-Free Electrolyte for Use in Rechargeable Magnesium Batteries. *Angew. Chem., Int. Ed.* **2015**, *54*, 7900−7904.

(5) McArthur, S. G.; Jay, R.; Geng, L.; Guo, J.; Lavallo, V. Below the 12-Vertex: 10-Vertex Carborane Anions as Non-Corrosive, Halide Free, Electrolytes for Rechargeable Mg Batteries. *Chem. Commun.* **2017**, *53*, 4453−4456.

(6) Zhao-Karger, Z.; Liu, R.; Dai, W.; Li, Z.; Diemant, T.; Vinayan, B. P.; Bonatto Minella, C.; Yu, X.; Manthiram, A.; Behm, R. J.; Ruben, M.; Fichtner, M. Toward Highly Reversible Magnesium-Sulfur Batteries with Efficient and Practical $Mg[B(Hfip)_4]_2$ Electrolyte. *ACS Energy Lett.* **2018**, *3*, 2005−2013.

(7) Chusid, O.; Gofer, Y.; Gizbar, H.; Vestfrid, Y.; Levi, E.; Aurbach, D.; Riech, I. Solid-State Rechargeable Magnesium Batteries. *Adv. Mater.* **2003**, *15*, 627−630.

(8) Thelen, J. L.; Inceoglu, S.; Venkatesan, N. R.; Mackay, N. G.; Balsara, N. P. Relationship between Ion Dissociation, Melt Morphology, and Electrochemical Performance of Lithium and Magnesium Single-Ion Conducting Block Copolymers. *Macromolecules* **2016**, *49*, 9139−9147.

(9) Girish Kumar, G.; Munichandraiah, N. Solid-State Rechargeable Magnesium Cell with Poly(Vinylidenefluoride)-Magnesium Triflate Gel Polymer Electrolyte. *J. Power Sources* **2001**, *102*, 46−54.

(10) Pandey, G. P.; Agrawal, R. C.; Hashmi, S. A. Performance Studies on Composite Gel Polymer Electrolytes for Rechargeable Magnesium Battery Application. *J. Phys. Chem. Solids* **2011**, *72*, 1408−1413.

(11) Kumar, G. G.; Munichandraiah, N. A Gel Polymer Electrolyte of Magnesium Triflate. *Solid State Ionics* **2000**, *128*, 203−210.

(12) Plancha, M. J. C. Characterisation and Modelling of Multivalent Polymer Electrolytes. In *Polymer Electrolytes: Fundamentals and Applications*; Elsevier: 2010; p 340.

(13) Bakker, A.; Gejji, S.; Lindgren, J.; Hermansson, K.; Probst, M. M. Contact Ion Pair Formation and Ether Oxygen Coordination in the Polymer Electrolytes $M[N(CF_3SO_2)_2]_2PEO_n$ for M = Mg, Ca, Sr and Ba. *Polymer* **1995**, *36*, 4371−4378.

(14) Girish Kumar, G.; Munichandraiah, N. Poly-(Methylmethacrylate) - Magnesium Triflate Gel Polymer Electrolyte for Solid State Magnesium Battery Application. *Electrochim. Acta* **2002**, *47*, 1013−1022.

(15) Morita, M.; Shirai, T.; Yoshimoto, N.; Ishikawa, M. Ionic Conductance Behavior of Polymeric Gel Electrolyte Containing Ionic Liquid Mixed with Magnesium Salt. *J. Power Sources* **2005**, *139*, 351−355.

(16) Rajput, N. N.; Qu, X.; Sa, N.; Burrell, A. K.; Persson, K. A. The Coupling between Stability and Ion Pair Formation in Magnesium Electrolytes from First-Principles Quantum Mechanics and Classical Molecular Dynamics. *J. Am. Chem. Soc.* **2015**, *137*, 3411−3420.

(17) Jay, R.; Tomich, A. W.; Zhang, J.; Zhao, Y.; De Gorostiza, A.; Lavallo, V.; Guo, J. A Comparative Study of Mg $(CB_{11}H_{12})_2$ and Mg

DOI: 10.1021/acsaem.9b00991
ACS Appl. Energy Mater. 2019, 2, 6355−6363

$(TFSI)_2$ at the Magnesium/Electrolyte Interface. *ACS Appl. Mater. Interfaces* **2019**, *11*, 11414−11420.
(18) Manjuladevi, R.; Thamilselvan, M.; Selvasekarapandian, S.; Mangalam, R.; Premalatha, M.; Monisha, S. Mg-Ion Conducting Blend Polymer Electrolyte Based on Poly (Vinyl Alcohol)-Poly (Acrylonitrile) with Magnesium Perchlorate. *Solid State Ionics* **2017**, *308*, 90−100.
(19) Polu, A. R.; Kumar, R.; Rhee, H. W. Effect of Ceramic Fillers on Polyethylene Glycol-Based Solid Polymer Electrolytes for Solid-State Magnesium Batteries. *High Perform. Polym.* **2014**, *26*, 628−631.
(20) Oh, J. S.; Ko, J. M.; Kim, D. W. Preparation and Characterization of Gel Polymer Electrolytes for Solid State Magnesium Batteries. *Electrochim. Acta* **2004**, *50*, 903−906.
(21) Kumar, G. G.; Munichandraiah, N. Reversibility of Mg/Mg^{2+} Couple in a Gel Polymer Electrolyte. *Electrochim. Acta* **1999**, *44*, 2663−2666.
(22) Shao, Y.; Rajput, N. N.; Hu, J.; Hu, M.; Liu, T.; Wei, Z.; Gu, M.; Deng, X.; Xu, S.; Han, K. S.; Wang, J.; Nie, Z.; Li, G.; Zavadil, K. R.; Xiao, J.; Wang, C.; Henderson, W. A.; Zhang, J. G.; Wang, Y.; Mueller, K. T.; Persson, K.; Liu, J. Nanocomposite Polymer Electrolyte for Rechargeable Magnesium Batteries. *Nano Energy* **2015**, *12*, 750−759.
(23) Mohtadi, R.; Matsui, M.; Arthur, T. S.; Hwang, S. J. Magnesium Borohydride: From Hydrogen Storage to Magnesium Battery. *Angew. Chem., Int. Ed.* **2012**, *51*, 9780−9783.
(24) Shao, Y.; Liu, T.; Li, G.; Gu, M.; Nie, Z.; Engelhard, M.; Xiao, J.; Lv, D.; Wang, C.; Zhang, J. G.; Liu, J. Coordination Chemistry in Magnesium Battery Electrolytes: How Ligands Affect Their Performance. *Sci. Rep.* **2013**, *3*, 3130.
(25) Rajput, N. N.; Seguin, T. J.; Wood, B. M.; Qu, X.; Persson, K. A. Elucidating Solvation Structures for Rational Design of Multivalent Electrolytes—A Review. *Topics in Current Chemistry* **2018**, *376*, 19.
(26) Barile, C. J.; Nuzzo, R. G.; Gewirth, A. A. Exploring Salt and Solvent Effects in Chloride-Based Electrolytes for Magnesium Electrodeposition and Dissolution. *J. Phys. Chem. C* **2015**, *119*, 13524−13534.
(27) Zhao-Karger, Z.; Gil Bardaji, M. E.; Fuhr, O.; Fichtner, M. A New Class of Non-Corrosive, Highly Efficient Electrolytes for Rechargeable Magnesium Batteries. *J. Mater. Chem. A* **2017**, *5*, 10815−10820.
(28) Luo, J.; Bi, Y.; Zhang, L.; Zhang, X.; Liu, T. L. A Stable, Non-Corrosive Perfluorinated Pinacolatoborate Mg Electrolyte for Rechargeable Mg Batteries. *Angew. Chem., Int. Ed.* **2019**, *58*, 6967−6972.
(29) Lau, C.-K.; Seguin, T. J.; Carino, E. V.; Hahn, N. T.; Connell, J. G.; Ingram, B. J.; Persson, K. A.; Zavadil, K. R.; Liao, C. Widening Electrochemical Window of Mg Salt by Weakly Coordinating Perfluoroalkoxyaluminate Anion for Mg Battery Electrolyte. *J. Electrochem. Soc.* **2019**, *166*, A1510−A1519.
(30) Du, A.; Zhang, H.; Zhang, Z.; Zhao, J.; Cui, Z.; Zhao, Y.; Dong, S.; Wang, L.; Zhou, X.; Cui, G. A Crosslinked Polytetrahydrofuran-Borate-Based Polymer Electrolyte Enabling Wide-Working-Temperature-Range Rechargeable Magnesium Batteries. *Adv. Mater.* **2019**, *31*, 1805930.
(31) Ford, H. O.; Merrill, L. C.; He, P.; Upadhyay, S. P.; Schaefer, J. L. Cross-Linked Ionomer Gel Separators for Polysulfide Shuttle Mitigation in Magnesium-Sulfur Batteries: Elucidation of Structure-Property Relationships. *Macromolecules* **2018**, *51*, 8629−8636.
(32) Elmore, C.; Seidler, M.; Ford, H.; Merrill, L.; Upadhyay, S.; Schneider, W.; Schaefer, J. Ion Transport in Solvent-Free, Cross-linked, Single-Ion Conducting Polymer Electrolytes for Post-Lithium Ion Batteries. *Batteries* **2018**, *4*, 28.
(33) Ma, Q.; Zhang, H.; Zhou, C.; Zheng, L.; Cheng, P.; Nie, J.; Feng, W.; Hu, Y. S.; Li, H.; Huang, X.; Chen, L.; Armand, M.; Zhou, A. Single Lithium-Ion Conducting Polymer Electrolytes Based on a Super-Delocalized Polyanion. *Angew. Chem., Int. Ed.* **2016**, *55*, 2521−2525.
(34) Meziane, R.; Bonnet, J. P.; Courty, M.; Djellab, K.; Armand, M. Single-Ion Polymer Electrolytes Based on a Delocalized Polyanion for Lithium Batteries. *Electrochim. Acta* **2011**, *57*, 14−19.
(35) Zhang, H.; Li, C.; Piszcz, M.; Coya, E.; Rojo, T.; Rodriguez-Martinez, L. M.; Armand, M.; Zhou, Z. Single Lithium-Ion Conducting Solid Polymer Electrolytes: Advances and Perspectives. *Chem. Soc. Rev.* **2017**, *46*, 797−815.
(36) Doyle, M.; Fuller, T. F.; Newman, J. G. The Importance of the Lithium Ion Transference Number in Lithium/Polymer Cells. *Electrochim. Acta* **1994**, *39*, 2073−2081.
(37) Merrill, L. C.; Schaefer, J. L. Conditioning-Free Electrolytes for Magnesium Batteries Using Sufone-Ether Mixtures with Increased Thermal Stability. *Chem. Mater.* **2018**, *30*, 3971−3974.
(38) Kang, S. J.; Lim, S. C.; Kim, H.; Heo, J. W.; Hwang, S.; Jang, M.; Yang, D.; Hong, S. T.; Lee, H. Non-Grignard and Lewis Acid-Free Sulfone Electrolytes for Rechargeable Magnesium Batteries. *Chem. Mater.* **2017**, *29*, 3174−3180.
(39) Tutusaus, O.; Mohtadi, R. Paving the Way towards Highly Stable and Practical Electrolytes for Rechargeable Magnesium Batteries. *ChemElectroChem.* **2015**, *2*, 51−57.
(40) Mandai, T.; Tatesaka, K.; Soh, K.; Masu, H.; Choudhary, A.; Tateyama, Y.; Ise, R.; Imai, H.; Takeguchi, T.; Kanamura, K. Modifications in Coordination Structure of Mg[TFSA]2-Based Supporting Salts for High-Voltage Magnesium Rechargeable Batteries. *Phys. Chem. Chem. Phys.* **2019**, *21*, 12100−12111.
(41) Rajput, N. N.; Qu, X.; Sa, N.; Burrell, A. K.; Persson, K. A. The Coupling between Stability and Ion Pair Formation in Magnesium Electrolytes from First-Principles Quantum Mechanics and Classical Molecular Dynamics. *J. Am. Chem. Soc.* **2015**, *137*, 3411−3420.
(42) Okoshi, M.; Yamada, Y.; Yamada, A.; Nakai, H. Theoretical Analysis on De-Solvation of Lithium, Sodium, and Magnesium Cations to Organic Electrolyte Solvents. *J. Electrochem. Soc.* **2013**, *160*, A2160−A2165.
(43) Senoh, H.; Sakaebe, H.; Sano, H.; Yao, M.; Kuratani, K.; Takeichi, N.; Kiyobayashi, T. Sulfone-Based Electrolyte Solutions for Rechargeable Magnesium Batteries Using 2,5-Dimethoxy-1,4-Benzoquinone Positive Electrode. *J. Electrochem. Soc.* **2014**, *161*, A1315−A1320.
(44) Doyle, M.; Lewittes, M. E.; Roelofs, M. G.; Perusich, S. A.; Lowrey, R. E. Relationship between Ionic Conductivity of Perfluorinated Ionomeric Membranes and Nonaqueous Solvent Properties. *J. Membr. Sci.* **2001**, *184*, 257−273.
(45) Kreuer, K. D.; Wohlfarth, A.; De Araujo, C. C.; Fuchs, A.; Maier, J. Single Alkaline-Ion (Li^+, Na^+) Conductors by Ion Exchange of Proton-Conducting Ionomers and Polyelectrolytes. *ChemPhysChem* **2011**, *12*, 2558−2560.
(46) de Molina, P. M.; Lad, S.; Helgeson, M. E. Heterogeneity and Its Influence on the Properties of Difunctional Poly(Ethylene Glycol) Hydrogels: Structure and Mechanics. *Macromolecules* **2015**, *48*, 5402−5411.
(47) Wang, J.-H. H.; Yang, C. H.-C.; Masser, H.; Shiau, H.-S.; O'Reilly, M. V.; Winey, K. I.; Runt, J.; Painter, P. C.; Colby, R. H. Ion States and Transport in Styrenesulfonate Methacrylic PEO_9 Random Copolymer Ionomers. *Macromolecules* **2015**, *48*, 7273−7285.
(48) Seitz, M. E.; Chan, C. D.; Opper, K. L.; Baughman, T. W.; Wagener, K. B.; Winey, K. I. Nanoscale Morphology in Precisely Sequenced Poly(Ethylene-Co-Acrylic Acid) Zinc Ionomers. *J. Am. Chem. Soc.* **2010**, *132*, 8165−8174.
(49) Hall, L. M.; Seitz, M. E.; Winey, K. I.; Opper, K. L.; Wagener, K. B.; Stevens, M. J.; Frischknecht, A. L. Ionic Aggregate Structure in Ionomer Melts: Effect of Molecular Architecture on Aggregates and the Ionomer Peak. *J. Am. Chem. Soc.* **2012**, *134*, 574−587.

DOI: 10.1021/acsaem.9b00991
ACS Appl. Energy Mater. 2019, 2, 6355−6363